

See discussions, stats, and author profiles for this publication at: <https://www.researchgate.net/publication/216670405>

Phosphorylation of Intrinsically Disordered Starmaker Protein Increases Its Ability To Control the Formation of Calcium Carbonate Crystals

ARTICLE *in* CRYSTAL GROWTH & DESIGN · JANUARY 2012

Impact Factor: 4.89 · DOI: 10.1021/cg200905f

CITATIONS

6

READS

45

4 AUTHORS, INCLUDING:



[Magdalena Wojtas](#)

Wroclaw University of Technology

7 PUBLICATIONS 31 CITATIONS

[SEE PROFILE](#)



[Piotr Dobryszycki](#)

Wroclaw University of Technology

39 PUBLICATIONS 229 CITATIONS

[SEE PROFILE](#)

Phosphorylation of Intrinsically Disordered Starmaker Protein Increases Its Ability To Control the Formation of Calcium Carbonate Crystals

Magdalena Wojtas,[†] Marek Wołczyk,[‡] Andrzej Ozyhar,[†] and Piotr Dobryszycki^{*†}

[†]Department of Biochemistry, Wrocław University of Technology, Wrocław, Poland

[‡]Institute of Low Temperature and Structure Research, Polish Academy of Sciences, Wrocław, Poland

ABSTRACT: The inner ear of the *Danio rerio* fish contains biominerals called otoliths that are composed of calcium carbonate crystals and a protein organic matrix. It has been previously suggested that Starmaker (Stm), which is an intrinsically disordered protein, acts as a component of otoliths that controls the size, shape, and polymorph of crystals. In this study, an in vitro calcium carbonate crystallization system was established to examine the role of Stm and extensively phosphorylated Stm (StmP) in the formation of crystals. SEM and X-ray diffraction analyses indicated that the dimensions of calcite crystals growing in the presence of Stm that had been phosphorylated by CK2 (StmP) were smaller in comparison with those growing with Stm. The shape of crystals growing in the presence of StmP were smoother and more spherical than those obtained in the presence of Stm. The decrease in crystal size, depending on the level of protein concentration, indicates that Stm and StmP act as inhibitors of crystal growth.

■ INTRODUCTION

Otoconia and otoliths are mineral deposits, which are responsible for sensing gravity and detecting linear acceleration. Otoconia are numerous and minute crystalline particles associated with an organic matrix, present in the gravity receptors of most vertebrates. Otoliths, which are located in the inner ear of fish, are calcified as a single mass, but also contain an organic matrix.¹ Both otoliths and otoconia are composed of calcium carbonates with a small fraction of organic molecules.^{1–3} Organic molecules act as a template for depositing crystals, promoting crystal growth in certain directions, and inhibiting crystal growth in undesired directions.⁴ These molecules are part of a rather heterogeneous population composed of proteins, glycoproteins, complex carbohydrates, proteoglycans, and glycosaminoglycans.⁴ Many organic matrix proteins are extremely acidic and have extensive post-translational modifications.⁵ Moreover, they often belong to the group of intrinsically disordered proteins (IDPs).^{6–9}

Starmaker (Stm) protein is a component of *Danio rerio* otoliths, which controls the size, shape, and polymorph of calcium carbonate crystals.¹⁰ Calcium carbonate crystallizes into three different polymorphs: rhombohedral calcite, the orthorhombic aragonite, and vaterite, which is hexagonal. It might also exist in an amorphous form.¹¹ All the polymorphic calcium carbonates may occur in biominerals. Under ambient conditions, depending on the amount of protein-mediated control, they may even develop simultaneously in two different forms.^{12,13} The well-formed otolith in *Danio rerio* is usually made up of aragonite; however, if Stm is absent, the otoliths are larger and are formed of calcite.¹⁰ Stm is a highly acidic protein rich in aspartyl (25%) and glutamyl (11%) residues, which might give it a predisposition to bind a large number of calcium ions and interact with calcium carbonate crystals.^{10,14} Stm also contains many seryl residues (19.5%). Bioinformatic tools (Disphos 1.3, NetPhos 2.0) predicted that almost all these residues could be phosphorylated.¹⁰ The unusual

amino acid composition results in the extended, rod-shaped conformation of the Stm molecule, which undergoes compaction in the presence of calcium ions.¹⁴ It has been previously shown in our laboratory that Stm, just like other proteins responsible for biomineral formation, is a member of the IDP group^{14,15} (for reviews, see refs 16 and 17). IDPs might exist as a heterogeneous population of molecules in several different conformational states. They can bind multiple ligands, and this may trigger ligand-dependent conformational changes which often lead to a less-extended and more-ordered structure.¹⁸ Stm, like other IDPs, has no well-defined tertiary structure. It has extraordinary structural flexibility and plasticity, so that the extended structure can undergo compaction in the presence of calcium ions. Calcium ions appear to be putative ligands of Stm.^{10,14,15}

The binding ability of counterions might be significantly amplified when a protein is post-translationally modified. In particular, phosphorylation seems to be crucial in order for metal ions to bind.^{5,19} There are some well-documented examples which have shown that phosphorylated proteins are engaged in biomineral formation. Phosphorylation is a crucial process which modulates biomineralization activity. For example, one analysis of the phosphates in the dentin matrix showed that there was a significant increase in the total content of phosphates during the development and maturation of dentin.²⁰ Another example of the effect of phosphorylation on biomineralization is dentin sialophosphoprotein (DSPP) in mammals, probably the closest functional analogue of Stm. DSPP gives rise to two mature products, dentin phosphoprotein (also named phosphophoryn) (DPP) and dentin sialoprotein (DSP), which are components of the calcified matrix of bones and teeth.²¹ It has been previously

Received: July 15, 2011

Revised: November 11, 2011

Published: November 11, 2011

shown that the phosphorylation of DPP is crucial for it to be able to function as a mediator of biominerization. At least 75% of DPP sequences (isolated from dentin) are seryl and aspartyl residues, and 85–90% of seryl residues are phosphorylated.^{5,22} The acidic and phosphoseryl residues (SerP) are largely present in repeating sequences of Asp-SerP-SerP or Asp-SerP.¹⁹ The Stm sequence contains similar repeats,¹⁰ but phosphorylation and the effect of phosphorylation on the Stm function has not been studied until now. Phosphorylation of DPP increases the binding capacity of calcium ions and induces a conformational transition of the extended protein molecule structure to a more compact one when in the presence of calcium ions. Consequently, phosphorylated DPP exhibits higher biominerization activity.⁹ Interestingly, phosphorylated DPP bound to collagen actively promotes hydroxyapatite-seeded crystal growth, while the dephosphorylated DPP–collagen complex greatly decreases the rate of crystal growth.²³ Osteopontin (OPN), which is a secretory glycoprotein rich in acidic and seryl residues, is another interesting protein that is involved in biominerization. It is prevalent in bone and is also present in brain, kidney, inner ear, and body fluids (milk, urine).²⁴ OPN is a major protein component of eggshells, which contain calcium carbonate.²⁵ The degree of OPN phosphorylation depends on the protein source and has different effects on hydroxyapatite formation and growth.^{26,27} Another highly acidic, bone- and teeth-specific protein, dentin matrix protein 1 (DMP1) has a dual function. Unphosphorylated DMP1 is localized in the nucleus, where it acts as a transcriptional component for the activation of matrix genes involved in mineralized tissue formation. On the other hand, calcium ions released from intracellular stores bind DMP1 and induce a DMP1 conformational change leading to phosphorylation by casein kinase 2 (CK2). Finally, phosphorylated protein is exported to the extracellular matrix, where it acts as a nucleator of hydroxyapatite.²⁸ A capacity for binding calcium, which is clearly related to phosphorylation in a manner similar to that with bone and dentin phosphoproteins, was also reported for orceinstein, an invertebrate matrix protein present in crustaceans. This highly acidic protein is involved in calcium carbonate storage in gastroliths. It binds calcium ions when it is phosphorylated; however, the dephosphorylated form does not appear to be involved in any calcium-binding activity.¹¹ The existence of numerous acidic phosphoproteins was also observed in chicken eggshells,²⁹ sea urchin shells, and the tooth matrix.³⁰ All the examples presented above strongly support the thesis that phosphorylation plays a crucial role in mediating the process of biominerization. This raised the question about the relationship between particular kinases and their corresponding biominerization activity. Most of the proteins mentioned above, including Stm, display a consensus sequence for casein kinases 1 and 2 (CK1 and CK2). It has also been shown that these kinases phosphorylate many of these proteins.^{19,26} Suzuki et al. showed CK2-like enzyme activity in the extracellular matrix of bone and dentin.³¹ Interestingly, casein kinase in Golgi apparatus is not only involved in the phosphorylation of OPN but seems to be the main physiological agent of it.³²

The process of mineral formation is too complex to be described quantitatively at the molecular level without simplified models that allow for an exploration of key biominerization factors. Therefore, we established a simple *in vitro* assay to describe the biominerization activity for Stm, based on observing the growth of calcium carbonate crystals.^{33–37} The aim of this work is to analyze the relationship between the degree of Stm

phosphorylation and the resulting biominerization activity. This work shows that CK2, PKA, and GSK3β phosphorylate Stm. We also analyzed different concentrations of protein and calcium ions and the resulting effect on the size, shape, and polymorphic form of the calcium carbonate crystals. We have demonstrated that crystal growth is controlled by Stm, that calcium carbonate crystal growth is inhibited by Stm, depending on the concentration of protein and calcium ions, and that phosphorylation by CK2 significantly increases the inhibiting effects of Stm.

MATERIALS AND METHODS

Protein Preparation. Recombinant, nontagged Stm protein without a signal peptide was obtained as previously described.¹⁵ Briefly, Stm was overexpressed in BL21(DE3) pLysS *E. coli* cells (Novagen, Germany), purified to homogeneity with a three-step procedure: fractionation with solid $(\text{NH}_4)_2\text{SO}_4$, gel filtration, and hydroxyapatite chromatography. Stm was stored in buffer A (10 mM Tris-HCl, 100 mM NaCl, 10% v/v glycerol, pH 7.0) at –80 °C.

Analytical Gel Filtration. Analytical gel filtration was performed as has been described previously,^{14,15} to calculate the hydrodynamic radius of Stm and StmP. Samples of Stm/StmP at a concentration of 0.3 mg/mL were loaded with a total volume of 100 μL onto a Superdex 200 10/300 GL column (Amersham Biosciences), connected to the AKTAexplorer system, and equilibrated with buffer A at a flow rate of 0.5 mL/min. The column was calibrated using the following standard proteins: thyroglobulin (85 Å), apoferritin (67 Å), catalase (52 Å), bovine serum albumin (35.5 Å), ovalbumin (30.5 Å), chymotrypsinogen (20.9 Å), myoglobin (20.2 Å), and cytochrome c (17 Å). The elution volume of each protein was used to calculate partition coefficients, K_{AV} , which were then plotted against the corresponding Stokes radii. The calculated K_{AV} was then fitted to the standard curve, and the Stokes radius of Stm was estimated.

In Vitro Phosphorylation Assay. *In vitro* phosphorylation of recombinant Stm was carried out using three different protein kinases: protein kinase A (PKA), a catalytic subunit from bovine hearts (Sigma, Poland); His-tagged, human glycogen synthase kinase-3 β (GSK-3β) (Sigma, Poland); an α-subunit of human recombinant casein kinase 2 (CK2) (Jena Bioscience, Germany). In each case, 5 μg of purified Stm was incubated with a defined amount of the appropriate kinase. Reactions with 6.2 U of PKA or 8 U of GSK-3β were performed in 25 mM Tris-HCl, 10 mM MgCl₂, 100 mM KCl, 100 μM ATP (2 μCi of [γ -³²P]ATP), 1 mM DTT, pH 7.0 for 1 h at 30 °C. Reactions with 33 μU of CK2 were performed in 20 mM Tris-HCl, 10 mM MgCl₂, 50 μM ATP (2 μCi of [γ -³²P]ATP), 1 mM DTT, pH 7.0 for 1 h at 37 °C. The reactions were terminated by the addition of a 4 × SDS sample buffer.³⁸ Samples were denatured at 95 °C for 10 min prior to protein separation by SDS-PAGE according to Laemmli and stained with Coomassie Brilliant Blue R 250 dye.³⁸ After SDS-PAGE separation, gels were dried in a vacuum at 80 °C and exposed to Imaging Plates (Fuji Photo Film). Fluorescence signals were scanned with the Fuji Film FLA-3000 Fluorescent Image Analyzer (Raytest Isotopenmeßgeräte GmbH).

Phosphorylation of Stm by CK2. Phosphorylation of Stm protein was carried out using CK2. One milligram of purified Stm was incubated with 6.6 mU of CK2 in buffer A, containing 50 μM ATP and 10 mM MgCl₂ for 1 h at 37 °C. Then, the mixture was dialyzed against buffer A to remove ATP and MgCl₂. Stm that was phosphorylated by CK2 is denoted as StmP in this work.

In Vitro Calcium Carbonate Mineralization Assay. The impact of Stm and StmP on the growth of calcium carbonate crystals was investigated using 96-well tissue culture plates (300 μL of assay volume per well). Thirty microliters of protein (final concentrations of 10, 50, 100 μg/mL), diluted in buffer A, was incubated with CaCl₂ (final

concentrations of 1, 10, 20 mM). Control experiments were performed under the same conditions, except that either trypsin (diluted in buffer A) in a 100 $\mu\text{g}/\text{mL}$ concentration or buffer A (a control to prove that glycerol and Tris did not influence the assay results) was added in place of Stm. Calcium carbonate crystals were grown inside a closed desiccator for 24 h at room temperature, and a slow diffusion of gases was released by the decomposition of ammonium carbonate placed at the bottom of the desiccator. Ten grams of solid ammonium carbonate was used. Finally, the crystallization solution was removed, and crystals were rinsed gently with 96% ethanol and water and air-dried at room temperature.

Morphology and Polymorph Analysis. SEM, Polarized Light Microscopy and X-ray Powder Diffraction Experiments. The morphology (size and shape) of the calcium was analyzed with scanning electron microscopy (SEM) using a JEOL JSM-5800LV scanning microscope at 15 kV after coating samples with gold. The size of the calcium carbonate crystals was determined from SEM images by measuring crystals for their edge length or diameter, in the case of hexagonal and spherical crystals, respectively. The crystals were also observed with a polarized light microscope (Olympus SZX10) to reveal the polycrystalline or monocrystalline character of the calcite crystals. The polymorphic forms of the calcium carbonate crystals were determined by X-ray powder diffractometry. Powder samples were measured with a PANalytical X'Pert X-ray powder diffractometer equipped with a focusing mirror and PIXcel solid-state linear detector. X-ray diffraction diagrams were registered with Cu K_{α} radiation ($\lambda = 0.15418 \text{ nm}$) using transmission geometry. A continuous scan in the $\theta/2\theta$ mode was applied in the 2θ range of 10–70° with the detector step size set to 0.013°. The total measurement time of an individual diagram was 29 min. Powder samples, formed as thin films, were put between two Kapton foils and fixed with a small amount of neutral grease. Samples were rotated with a revolution time of 1 s.

Fluorescence Experiments. Stm, StmP, and trypsin in the concentration of 20 μM were incubated with a 10-fold molar excess of AlexaFluor 488 (Invitrogen) in buffer A for 2 h at 24 °C in the dark. Unreacted AlexaFluor 488 was removed by size-exclusion chromatography using a Superdex 200 10/300 GL column connected to the AKTAexplorer system (Amersham Biosciences). The labeled proteins were concentrated to about 1.0 mg/mL using an Amicon Ultra-4 Centrifugal Filter Unit (Millipore). Protein concentration was determined by the Lowry method.³⁹ The in vitro calcium carbonate mineralization assay was performed in the presence of the labeled proteins as described above.

RESULTS

The Phosphorylation of Stm. As discussed above, proteins involved in biominerization are often highly phosphorylated, and it is well documented that this chemical modification significantly affects biological functions. At the beginning of this study, Stm phosphorylation with different kinases was analyzed in silico and in vitro. Recombinant Stm is free of any post-translational modifications.^{14,15} However, there are a large number of putative phosphorylation sites in the Stm amino acid sequence. Disphos and NetPhos predicted 128 and 137, respectively, as the putative phosphorylation sites in the Stm sequence (data not shown). NetPhosK predictions led to the identification of numerous potential phosphorylation sites for several kinases (Figure 1A).

The most abundant were phosphorylation sites corresponding to the consensus sequences for CK1 and CK2. NetPhosK indicated 12 and 104 putative phosphorylation sites for CK1 and CK2, respectively, with a score above 0.5. A few of the consensus sequences for CK1 and CK2 overlap in the Stm sequence. Three sites were predicted for GSK3, while no phosphorylation site was

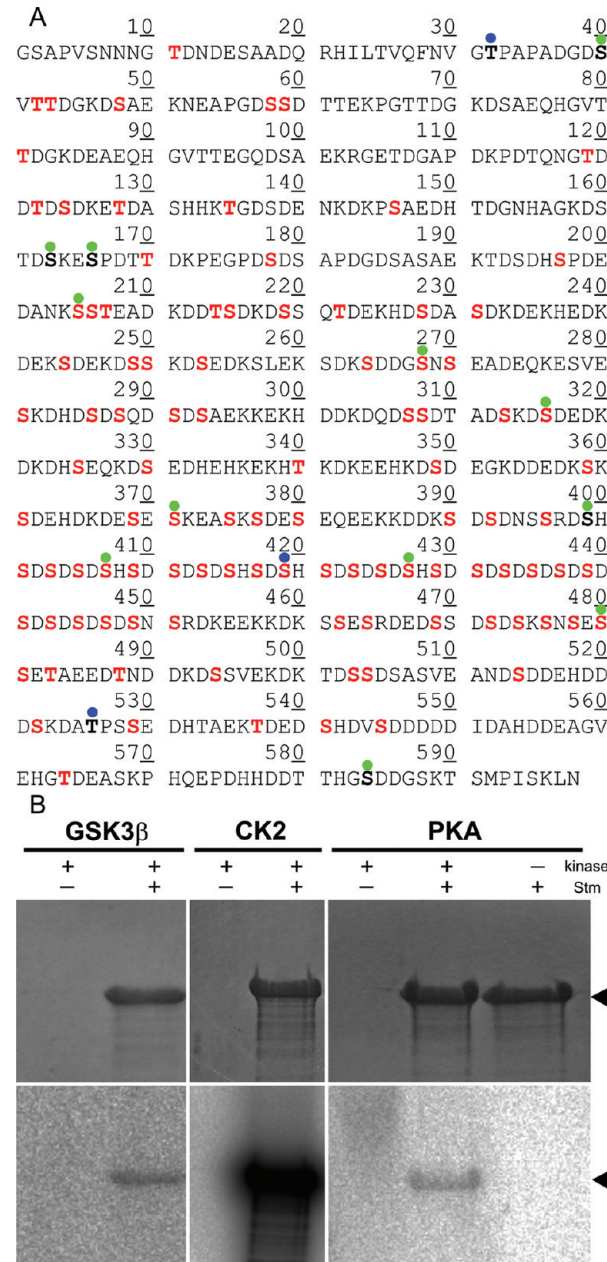


Figure 1. Stm undergoes phosphorylation. In silico and in vitro analysis. (A) Phosphorylation sites in the Stm protein sequence predicted by NetPhosK. All phosphorylation sites for CK1, CK2, and GSK3 β are highlighted in bold. Moreover, phosphorylation sites for GSK3 β , CK1, and CK2 are indicated by the blue dot, green dot, and red font, respectively. (B) In vitro phosphorylation of Stm was performed using GSK3 β , CK2, and PKA kinases. In each case, 5 μg of purified Stm was used. Reactions with 6.2 U of PKA or 8 U of GSK-3 β were performed in 25 mM Tris-HCl, 10 mM MgCl₂, 100 mM KCl, 100 μM ATP (2 μCi of [γ -³²P]ATP), 1 mM DTT, pH 7.0 for 1 h at 30 °C. Reactions with 33 μU of CK2 were performed in 20 mM Tris-HCl, 10 mM MgCl₂, 50 μM ATP (2 μCi of [γ -³²P]ATP), 1 mM DTT, pH 7.0 for 1 h at 37 °C. The top panel represents Coomassie dye-stained gel (to visualize protein), and the bottom panel represents autoradiogram (to visualize radioactivity from phosphate groups incorporated into Stm). The arrowheads indicate the position of Stm.

predicted for PKA. Several phosphorylation sites for other kinases were predicted by NetPhosK (data not shown), but only

PKA, CK2, and GSK3 β were examined experimentally. All investigated kinases were able to phosphorylate Stm in vitro (Figure 1B). Coomassie dye staining enables visualization of proteins regardless of phosphorylation (Figure 1B, top panel), whereas autoradiography (Figure 1B, bottom panel) indicates molecules that have been radioactively labeled. The band observed on the autoradiogram occurs only with phosphorylated Stm because of the incorporation of the ^{32}P -labeled phosphate group(s) by the respective kinase onto the Stm hydroxyl of the Ser or Thr residues. There was no band observed in the control electrophoresis in the absence of kinase or Stm. Qualitatively, the results correspond to the NetPhosK predictions, except for PKA, which was able to phosphorylate Stm in vitro. Limited phosphorylation was observed for GSK3 β and PKA, while CK2 caused hyperphosphorylation of Stm comparable to the hyperphosphorylation of histone H1 by the PKA (data not shown). In the gels stained with Coomassie dye there were some visible degradation products. These poorly visible bands of higher electrophoretic mobility were also observed for products of Stm phosphorylation by CK2. The level of phosphorylation of Stm by CK2 was checked after 5, 10, and 20 min. The signal in the autoradiography images observed after 5 min was almost as strong as after 1 h (data not shown).

The analytical gel filtration experiment has shown that an apparent Stokes radius of StmP of ca. 79 Å is almost the same in the experimental error range as the Stm radius. The above presented results characterize Stm as an IDP protein with hydroxyl residues that are exposed and ready for chemical modification and with molecule shape that does not change significantly.

Stm and StmP Change the Size and Morphology of Calcium Carbonate Crystals. Stm is required for the proper formation of otoliths, as Söllner et al. demonstrated;¹⁰ however, neither post-translational modifications of Stm nor the role of such modifications have been described until now. An in vitro calcium carbonate crystallization system was established to examine the extensive phosphorylation of Stm by CK2. Four parallel biomimetic experiments were performed in the presence of Stm, StmP (Stm phosphorylated by CK2), and trypsin (as a control protein not involved in biomimetication), and the last experiment without any protein at all.

Preliminary in vitro crystallization experiments were performed without rinsing the crystals with ethanol and water. We observed amorphous calcium carbonate and/or polymer-induced liquid precursor (PILP)^{40,41} (Figure 2). After washing the crystals with ethanol and water, only solid, crystalline particles were observed.

Calcium carbonate crystals grown in the presence of Stm and StmP (Figures 3 and 4) differed significantly in shape and size from the crystals obtained without any protein (Figure 5B,D,F), or in the presence of trypsin (Figure 5A,C, E). Note that all images in Figures 3–5 are in the same scale. The scale bar on the upper edge of each image represents a 10- μm distance, while the inset is 4× the magnification of the main image.

All the control crystals were prismatic in contrast to the crystals grown in the presence of Stm and StmP. With a 10 $\mu\text{g}/\text{mL}$ Stm concentration (Figure 3A,D,G), the crystal grains were mainly prismatic. A stairlike structure was also observed, especially with a higher concentration of calcium ions (Figure 3A,D,G, inset). When 50 $\mu\text{g}/\text{mL}$ of Stm was used, rounded crystals were predominant (Figure 3B,E,H). This result was the most visible with a 10 mM concentration of calcium ions (Figure 3E, inset), where spherical particles were abundant (Figure 3E, inset). With a 20 mM concentration of calcium ions, crystals had rounded

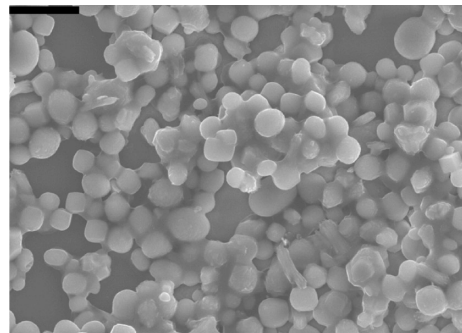


Figure 2. Amorphous calcium carbonate and/or polymer-induced liquid precursor (PILP). SEM images of calcium carbonate obtained in the presence of 100 $\mu\text{g}/\text{mL}$ Stm and 10 mM calcium ions. The scale bar on the upper edge of the image represents a 10 μm distance. Crystallization was performed without rinsing crystals with ethanol and water.

edges but were still prismatic (Figure 3H). With a 1 mM concentration of calcium ions, the observed crystals were prismatic, rounded, and elongated (Figure 3B). With a protein concentration of 100 $\mu\text{g}/\text{mL}$, Stm exhibited the greatest impact on crystal formation, as they were mostly in a spherical shape (Figure 3C,F,I). Only a few prismatic crystals were present with a 20 mM concentration of calcium ions (Figure 3I). Interestingly, the number of elongated crystals increased with a decrease in the calcium ion concentration. With a 1 mM concentration of calcium ions, nearly all the crystals were elongated (Figure 3C). At various concentrations, the observed impact of StmP was similar but definitely more pronounced than for Stm (Figure 4). Spherical crystals were observed even with a 10 $\mu\text{g}/\text{mL}$ protein concentration (Figure 4A, D, G). With a 50 $\mu\text{g}/\text{mL}$ concentration, most of the observed particles were spherical (Figure 4B,E,H). In the presence of 100 $\mu\text{g}/\text{mL}$ of StmP, elongated crystals appeared (Figure 4C,F,I), and they were especially apparent with 1 mM of calcium ions (Figure 4C, inset). At a 10 and 20 mM calcium ion concentration, the crystals were spherical, resembling elongated ovals, and they were much smoother (Figure 4F,I).

Figure 6 and Table 1 shows a comparison of the crystal sizes. It is clear that Stm and StmP dramatically decreased the dimensions of the crystals in comparison with crystals obtained in the presence of trypsin or in the absence of any protein. The degree of impact depended on the concentration of Stm or StmP. StmP decreased the size of the crystals much more than Stm did (Figure 6A,B). In the absence of Stm or StmP, the size of the calcium carbonate crystals depended greatly on the calcium ion concentration, becoming larger with increasing concentrations of calcium ions (Figure 6, no protein and trypsin). This same effect was less evident for Stm than for StmP.

Note that the calcium ion concentration had a greater effect on the size of the crystals in the presence of Stm than in the presence of StmP, which indicates that StmP is a stronger inhibitor of crystal growth. Moreover, there was a wide range of crystal dimensions obtained for the control groups in the presence of trypsin or in the absence of any protein in comparison with the rather narrow range of crystal sizes grown in the presence of Stm and StmP (Figure 6). For example, 100 $\mu\text{g}/\text{mL}$ trypsin with 20 mM calcium ions generated crystals with an edge length ranging from 45 to 80 μm , while Stm and StmP under the same conditions, generated crystals with diameters of 4–11 μm and 1–6 μm , respectively. Thus, Stm and StmP inhibit crystal growth and maintain a rather uniform crystal size for given

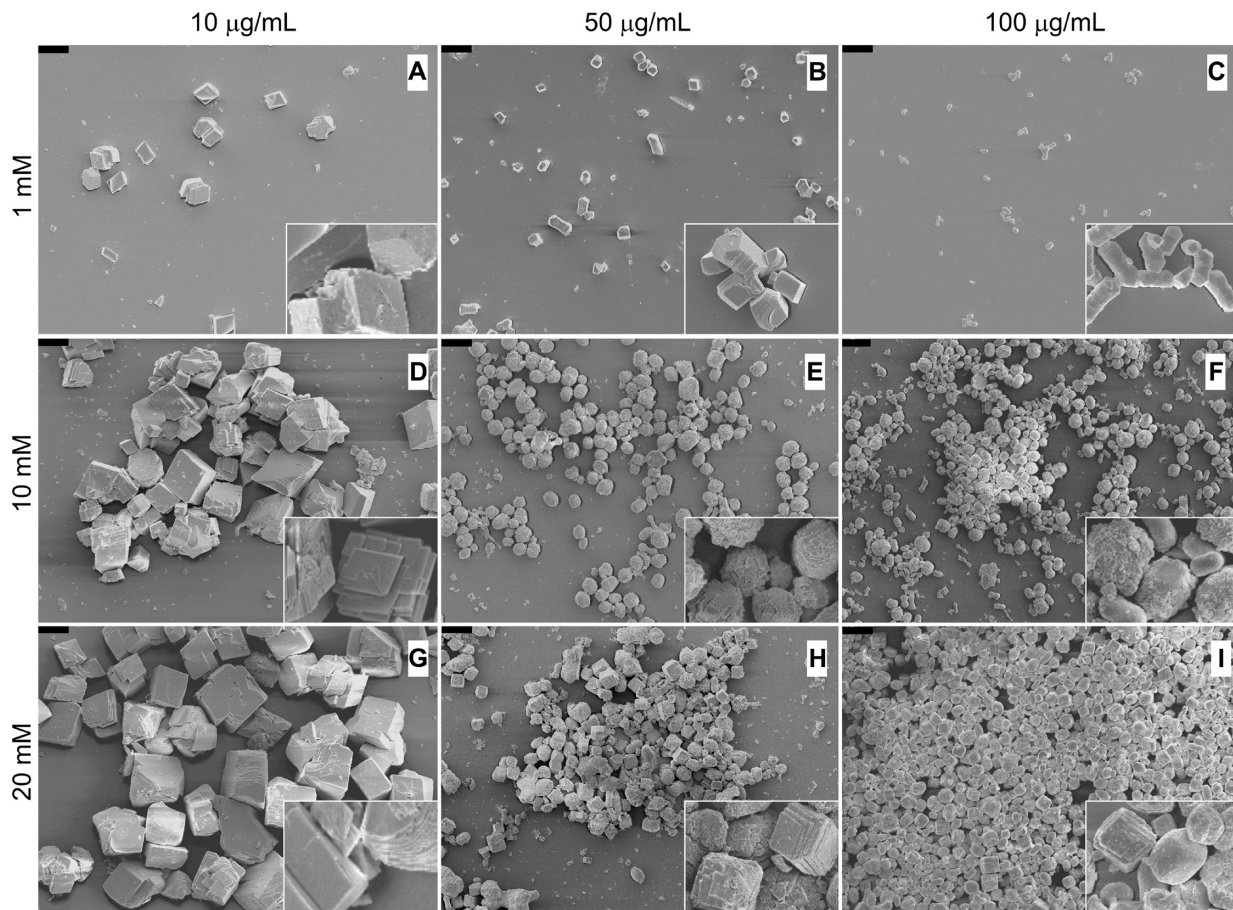


Figure 3. The effect of Stm on in vitro calcium carbonate crystallization. SEM images of calcium carbonate crystals grown in the presence of the Stm protein in the following concentrations: 10 µg/mL (A, D, G), 50 µg/mL (B, E, H), 100 µg/mL (C, F, I). Concentrations of calcium ions used: 1 mM (A–C); 10 mM (D–F); 20 mM (G–I). The scale bar on the upper edge of each image represents a 10-µm distance. Note that every single image contains an inset with higher magnification of the crystals (the inset is 4× the magnification of the main image). All images in Figures 3–5 are in the same scale.

concentrations of calcium ions. In addition, the observed effects were greater for StmP than for Stm.

Polarized light microscopy has shown that most Stm crystals are monocrystalline, but the twinning of two or more of crystals was also observed. All crystals exhibited birefringence (data not shown).

Effect of Stm and StmP on Polymorph Selection. The aim of our X-ray powder diffractometry experiments was to characterize the polymorph of calcium carbonate crystals from an in vitro biominerization assay. Diffraction diagrams obtained from calcium carbonate crystals grown in the presence of Stm and StmP indicate the existence of calcite (Figure 7A,B). Control crystals obtained in the absence of any protein or in the presence of trypsin exhibited polymorph heterogeneity (Figure 7C). Calcite was the most often observed polymorph; however, small amounts of vaterite and aragonite crystals were also present. Vaterite crystals were also observed with 10 µg/mL of Stm at a 10 mM calcium ion concentration (Figure 7A). It seems that in this case the protein concentration was too low to favor only calcite. However, vaterite crystals were not observed with 10 µg/mL Stm at a 1 mM calcium ion concentration. This observation can be explained as the result of the lower concentration of calcium chloride which caused slower crystal growth and, in turn, enabled Stm to exclusively favor calcite. Only calcite was observed in crystals grown in the presence of StmP, even at a

low protein concentration and 10 mM calcium chloride. Neither the aragonite nor the vaterite polymorph was observed for Stm or StmP with a protein concentration of 100 µg/mL.

Stm and StmP Are the Constituents of Calcium Carbonate Crystals. Stm from the inner ear of *Danio rerio* is a component of otoliths.¹⁰ To examine if recombinant Stm and StmP are able to interact with calcium carbonate crystal grains during an in vitro biominerization assay, proteins were labeled with the succinimidyl ester of the Alexa Fluor 488 dye at the amine end. Figure 8 shows the fluorescence images (A–C) and optical micrographs (D–F) of crystals obtained from the in vitro biominerization assay with 100 µg/mL protein and 10 mM calcium chloride. Fluorescence microscopy clearly demonstrated that Stm and StmP are constituents of crystals. All calcium carbonate crystals grown in the presence of Stm and StmP emitted green fluorescence. Similar results were obtained for the remaining protein concentrations (10, 50 µg/mL) and calcium ion concentrations (1, 20 mM) (data not shown). Fluorescently labeled trypsin (100 µg/mL), used as a control protein, did not affect the calcium carbonate crystals (Figure 8C, F).

■ DISCUSSION

To date, a few component proteins in otoliths have been identified.^{10,42–46} However, there is little information about

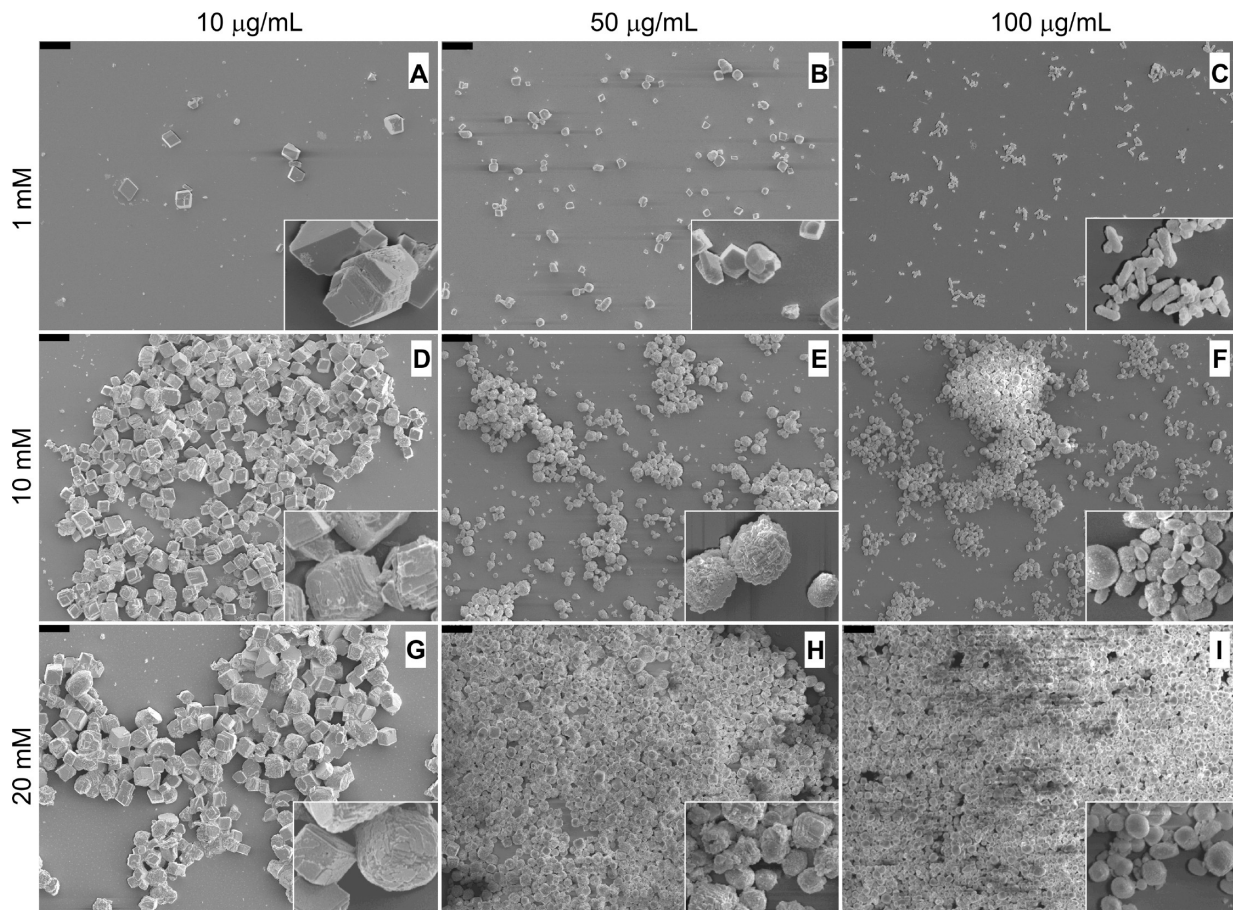


Figure 4. The effect of StmP on *in vitro* calcium carbonate crystallization. SEM images of calcium carbonate crystals grown in the presence of StmP protein in the following concentrations: 10 µg/mL (A, D, G); 50 µg/mL (B, E, H); 100 µg/mL (C, F, I). Concentrations of calcium ions used: 1 mM (A–C); 10 mM (D–F); 20 mM (G–I). All images in Figures 3–5 are in the same scale. The scale bar on the upper edge of each image represents a 10-µm distance. Note that every single image contains an inset which shows higher magnification of the crystals (inset is 4× the magnification of the main image).

what effect chemical modifications in such proteins has on calcium carbonate biominerization formation. To examine the role of phosphorylation, we analyzed the formation of calcium carbonate crystals in the presence of intrinsically disordered, recombinant Stm protein. Protein phosphorylation is involved in biominerization. It often occurs extensively on seryl and treonyl residues and is principally catalyzed by caseinlike kinase activity.^{5,19,26,31,47} The results obtained for the Stm protein correspond to these data. Stm is highly phosphorylated by CK2 and displays numerous phosphorylation sites for other kinases. Even PKA, which was not predicted by NetPhosK, was able to phosphorylate Stm. Although GSK3β sometimes requires introductory phosphorylated protein from another kinase,⁴⁸ unmodified Stm is a substrate for GSK3β as well. Stm's susceptibility to phosphorylation seems to be associated with its extended and flexible structure, which is characteristic for IDPs. The lack of a well-packed hydrophobic core and rapid fluctuations in the peptide chain lead to a greater amount of potential phosphorylation sites, more so than in the case of globular proteins. The immediate (after no more than 5 min) phosphorylation of Stm is additional support for the thesis that the disordered character of Stm facilitates post-translational modifications.⁴⁹ On the basis of previously published results^{9,11,19,23,26} we assume that such extensive phosphorylation can modulate the biominerization activity of the Stm protein.

Interestingly, the *starmaker* gene is not expressed exclusively in the inner ear of zebrafish, but also in the lateral line organ, where biominerals have not been observed.¹⁰ It is also known that some proteins involved in biominerization, such as DMP1 or OPN, display a wide range of phosphates, though they may fulfill various functions apart from biominerization.^{24,27,28}

In this paper, we have demonstrated the effect of phosphorylation on Stm's biominerization activity. *In vitro* biominerization experiments indicate that StmP has a greater effect on the size and morphology of calcium carbonate crystals than unphosphorylated Stm at all the tested calcium ion and protein concentrations. The dimensions of calcium carbonate crystals grown in the presence of StmP were always smaller in comparison with those grown with Stm. Also the shape of the crystals grown in the presence of StmP were more spherical and smoother in comparison to those obtained in the presence of Stm. These results led us to question how phosphorylation modulates Stm activity. First of all, it should be noted that Stm is rich in negatively charged amino acid residues, which results in strong electrostatic repulsion that is even more amplified by extensive phosphorylation. As mentioned earlier, phosphorylation frequently occurs in the repeating sequences of Asp-Ser-Ser or Asp-Ser.¹⁹ Thus, the presence of phosphoseryl residues in the proximity of aspartyl residues might extend the Stm molecule even further, as a result of the repulsion from the

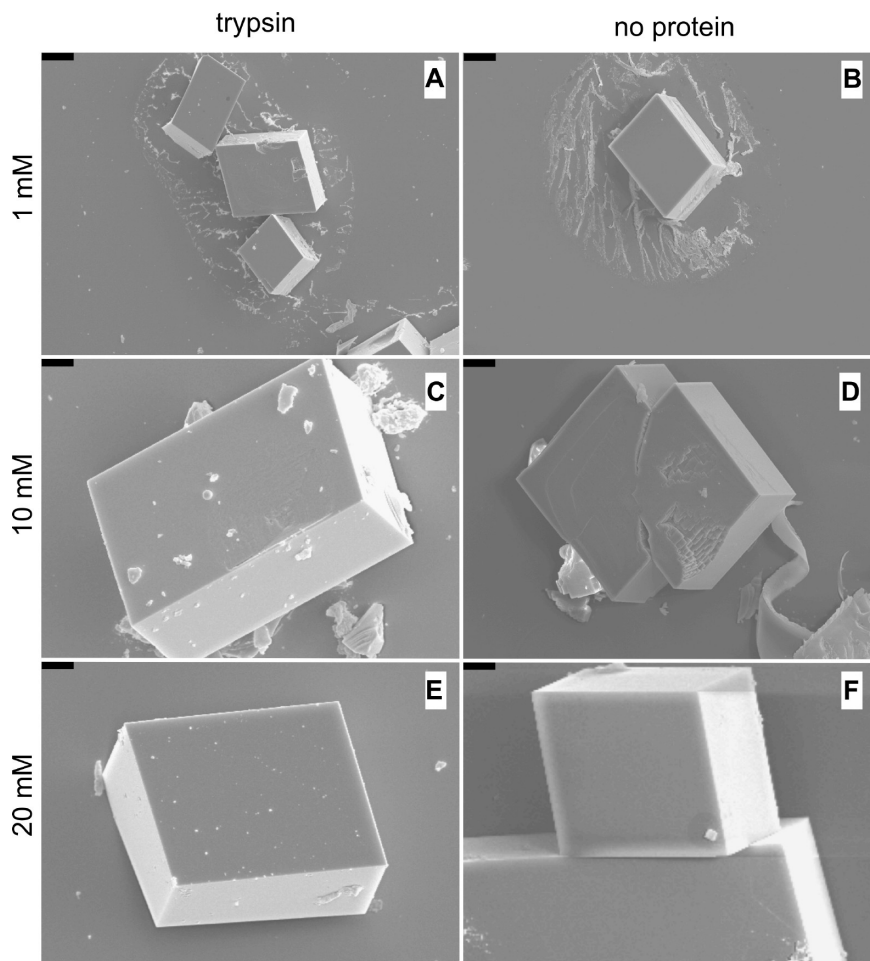


Figure 5. The effect of trypsin on in vitro calcium carbonate crystallization. SEM images of calcium carbonate crystals grown in the presence of trypsin in a concentration of 100 $\mu\text{g}/\text{mL}$ (A, C, E) and a negative control (no protein added) (B, D, F). The following concentrations of calcium ions were used: 1 mM (A, B); 10 mM (C, D); 20 mM (E, F). All images in Figures 3–5 are in the same scale. The scale bar on the upper edge of each image represents a 10- μm distance.

neighboring electrostatic group. This might stiffen the protein backbone somewhat and increase the polypeptide chain persistence length.⁵ The extended conformation of the protein backbone might lead to the placement of phosphate and carboxylate groups at regular intervals and result in the formation of properly spaced calcium-binding sites.⁵⁰ Although gel filtration experiments showed no significant differences in the hydrodynamic radius between Stm and StmP we cannot exclude the possibility that phosphorylation causes conformational changes in the Stm molecule. Moreover, conformational analysis of Asp-SerP-SerP or Asp-SerP repeats reveal that this sequence might assume a unique structure which can bind counterions.⁵ Analysis of the Stm sequences did not reveal canonical calcium-binding domains,⁵¹ thus, the mentioned interaction is possible.

Interestingly, Stm and StmP affect nucleation and they also interfere with crystal growth. The increased number of crystals in the presence of Stm/StmP might indicate that more nucleation sites are formed. The high negative charge of Stm and even more negatively charged StmP might cause calcium ions from the solution to gather and promote nucleation. Moreover, it is possible that Stm/StmP stabilizes liquid amorphous calcium carbonate, as was shown for the poly-Asp peptide or ovalbumin,^{40,41} because PILP and/or amorphous calcium carbonate was observed when

crystals were not washed with ethanol and water before the SEM experiment (Figure 2). It seems that the disordered structure of Stm/StmP facilitates the formation of liquid amorphous calcium carbonate because of the large extension of the backbone and better accessibility of charged groups.

Crystal habit indicates that Stm/StmP interferes with calcium carbonate growth. Calcite crystals are mostly monocrystals, so it seems possible that Stm/StmP acts as nucleator and then inhibits crystal growth. The decrease in the dimensions of calcium carbonate crystals, depending on the protein concentration used, indicates that Stm and StmP act as inhibitors of crystal growth. These data are in agreement with the data obtained for native Stm from *Danio rerio* otoliths.^{10,52} It has been previously suggested that the inhibitory effect of protein on crystal growth is related to the flexibility of the protein's backbone.^{7,53} It has been shown, for example, that the N-terminal fragment of CAP-1 inhibits crystal growth less efficiently, because it possesses a more ordered structure than the C-terminal fragment.⁵³ NMR studies have indicated that the N-terminal fragment of statherin strongly interacts through the phosphoseryl residues with the hydroxyapatite crystal, while the C-terminus is highly mobile. The mobility of the statherin C-terminus on the surface of the crystal can more effectively block nucleation sites than a rigidly bound protein.⁷

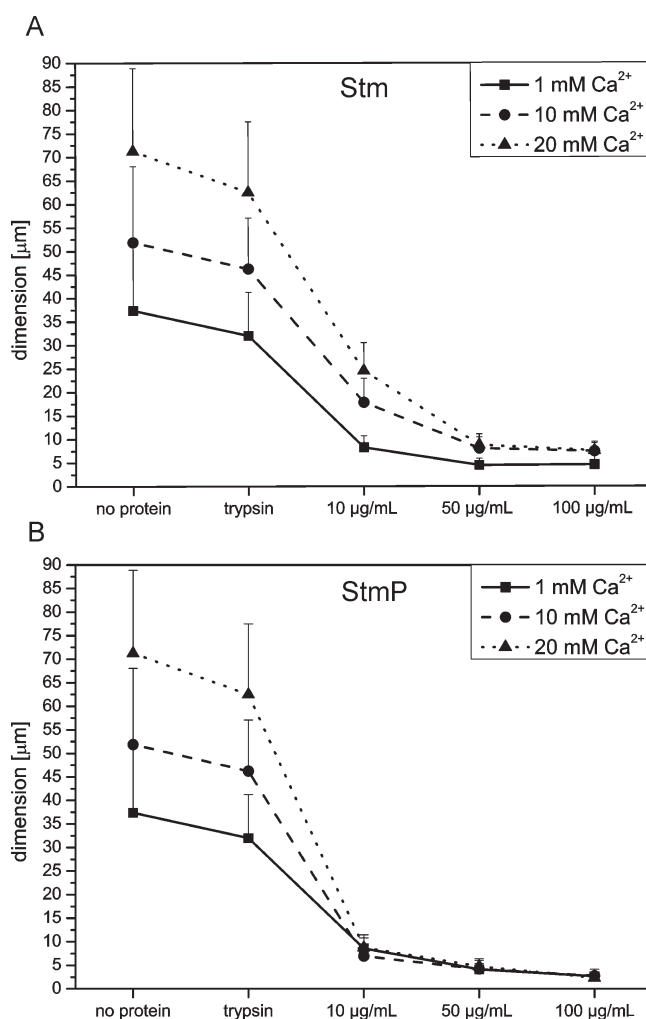


Figure 6. A comparison of the dimensions of calcium carbonate crystals obtained under different conditions. The average size of calcium carbonate crystals formed in the presence of Stm (A) and StmP (B). The size of the calcium carbonate crystals was determined from SEM images by measuring the crystal edge length or crystal diameter for hexagonal and spherical crystals, respectively. Note that for comparison, respective data obtained in the presence of trypsin at a concentration of 100 μg/mL and in the absence of any protein are shown in panels A and B. Calcium ion concentrations are represented by a solid line (1 mM), dashed line (10 mM), or dotted line (20 mM).

Table 1. Average Calcium Carbonate Crystal Size

protein (μg/mL)	Ca ²⁺ (mM)	average crystal size (μm)			
		Stm	StmP	trypsin	no protein
10	1	8.3	8.6		
	10	17.9	6.9		
	20	25.6	8.8		
50	1	4.5	4.1		
	10	8.1	4.2		
	20	8.8	4.8		
100	1	4.6	2.7	32.0	37.4
	10	7.4	2.8	46.3	51.9
	20	7.6	2.3	62.5	71.3

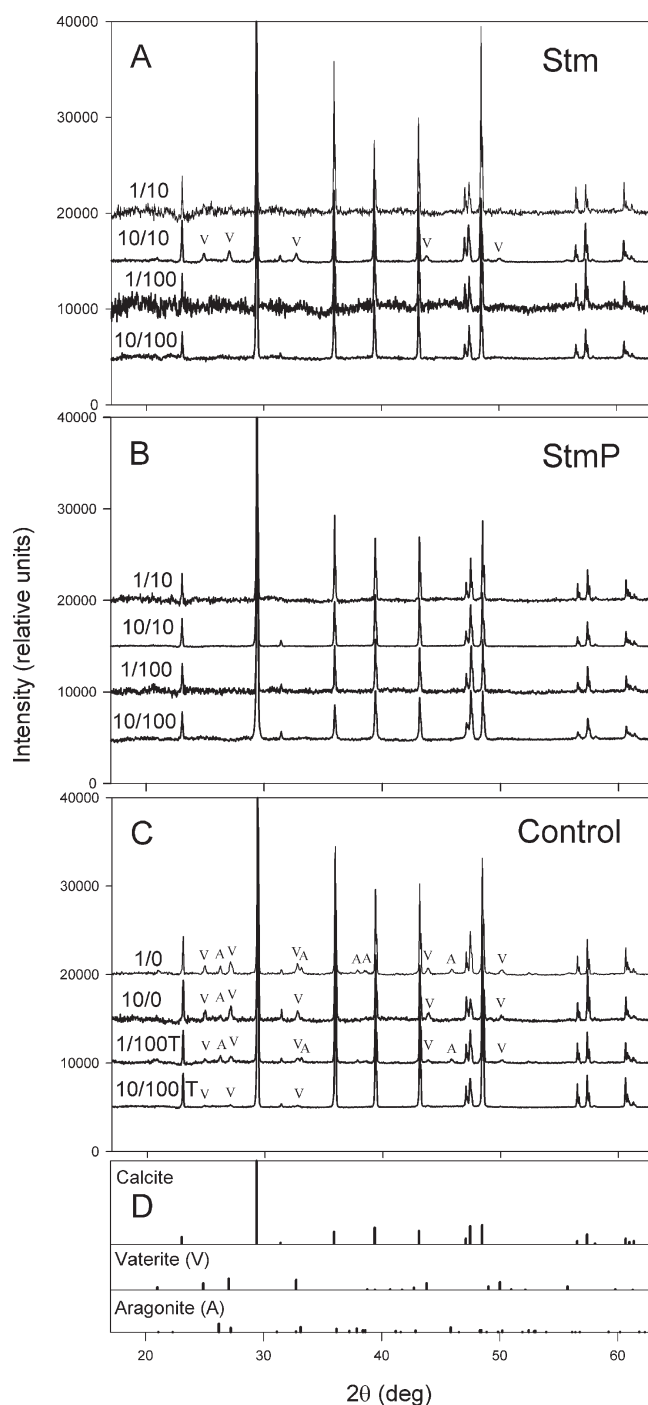


Figure 7. X-ray powder diffraction analysis of the calcium carbonate polymorph. X-ray powder diffraction diagrams obtained for three groups of samples: (A) samples crystallized in the presence of Stm protein; (B) crystallized in the presence of StmP protein; (C) control samples crystallized without the presence of protein or in the presence of trypsin. *m/n* symbol for each pattern describes the calcium ion concentration (mM)/protein concentration (μg/mL). Diagrams were rescaled to provide a comparable intensity level. Noisier plots resulted in a smaller signal, i.e., less crystal fractions were obtained during synthesis or were obtained having a lower degree of crystallinity. (D) Stick diagrams presenting the peak positions and intensities of ICDD standards for polymorphic forms of CaCO₃: calcite 47–1743, vaterite 33–0268, and aragonite 41–1475. The peaks of vaterite and aragonite minority phases are indicated in panels A and C by V and A, respectively.

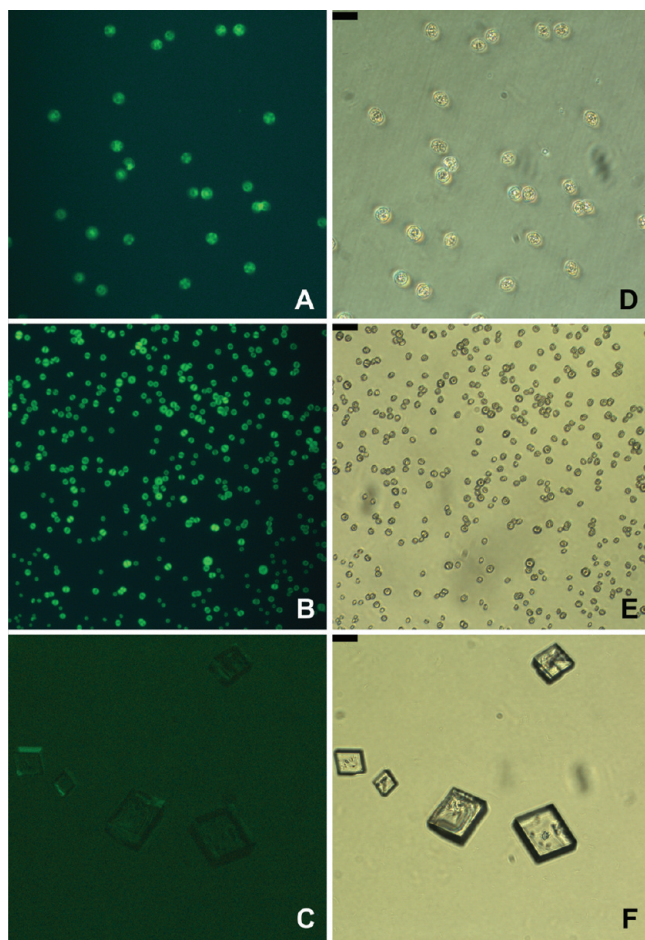


Figure 8. Fluorescence images and optical micrographs of calcium carbonate crystals. In vitro biominerization assay performed in the presence of proteins and calcium ion concentrations of 100 $\mu\text{g}/\text{mL}$ and 10 mM, respectively. A–C, fluorescent images; D–F, optical micrographs. A, D: crystals growing in the presence of Stm labeled with Alexa Fluor 488. B, E: crystals growing in the presence of StmP labeled with Alexa Fluor 488. C, F: crystals growing in the presence of trypsin labeled with Alexa Fluor 488.

It is possible that Stm, which is also highly disordered, may act in a similar mode.

Some calcite crystals growing in the presence of Stm/StmP are elongated, especially in the presence of high protein concentrations and low calcium ion concentrations (Figures 3 and 4). Possibly Stm and StmP have higher affinity to one crystal plane over the other. However, fluorescence microscopy images did not reveal any stronger emission from any plane (Figure 8). The preferential interactions between the proteins and the particular crystal faces or edges have been previously reported. The AP8 peptide from abalone shell nacre specifically affects the acute edges of the calcite faces.⁵⁴ The interaction causes rounding of the calcite edges similar to that observed in the presence of Stm/StmP (Figures 3 and 4). At higher Stm or StmP concentrations, all edges of the crystals are equally rounded and no specificity was observed (Figure 3 and 4). Calcite crystals growing in the presence of the n16 peptide from oyster shells do not retain any sharp corner features that lead to the formation of stairlike structures.³³ The n16 mode of action seems to be more similar to the effect from Stm at higher protein concentrations. The

different effects of Stm and StmP on crystal shapes seems to be dependent on the protein and calcium ion concentrations. This effect is more pronounced for StmP (Figure 4). Decreasing the calcium ion concentration also affected the crystal shape, leading to elongation of the crystals. All the observations described above indicate that Stm/StmP is multifunctional, which is typical for IDPs.

Acidic proteins involved in controlling the size and shape of crystals are also responsible for polymorph selection.⁵⁵ Our analysis of the crystal polymorphs revealed that recombinant Stm and StmP stabilize calcite. This was surprising, because *Danio rerio* otoliths consist of aragonite, and Stm directs the proper selection of the polymorph.¹⁰ However, it should be considered that endolymph is highly complex,^{2,3} and there is a delicate equilibrium between aragonite and calcite. Stm *in vivo* probably interacts with many molecules which modulate its function and facilitate proper polymorph selection. Moreover, the nucleation of a desired polymorph also requires an appropriate microenvironment.⁵⁶ In some cases aragonite growth was induced by magnesium ions.^{57,58} Magnesium ions bind water molecules more thoroughly compared to calcium ions. Mg²⁺ are only partially dehydrated when attached to growing crystals and inhibit calcite growth. The aragonite crystal lattice is denser than calcite; hence, partially dehydrated Mg²⁺ ions cannot be incorporated. Thus, at a high ratio of magnesium/calcium ions, aragonite is favored;^{59,60} however, in the absence of Stm, calcite otholiths are formed.¹⁰

Calcium carbonate biominerals are frequently composed of water-soluble, acidic proteins and framework macromolecules, such as collagen and chitin, which form a macromolecular scaffold. Data obtained for proteins extracted from mollusk shells indicated that proper polymorph selection requires more than one macromolecule.⁶¹ Mollusk shells consist of nacreous layers (aragonite crystals) or prismatic layers (calcite crystals). Organic matrixes were extracted from mollusk shells according to their solubility in EDTA and were classified as soluble and insoluble matrix proteins.⁵⁵ Soluble macromolecules extracted from nacre can induce aragonite, and macromolecules from the prism can induce calcite growth.¹³ However, it has been proven that other molecules such as silk-fibroin and β -chitin can also influence the type of polymorph.⁶¹ It has been shown that a mixture of soluble macromolecules, silk-fibroin, and β -chitin can induce the same crystal polymorph type as those from the prismatic or nacre layer. However, only calcite crystals were observed after using a mixture without silk-fibroin, regardless of whether the soluble macromolecules were extracted from nacreous or prismatic layers⁶¹ It should be noted that the experiments described above concerned a mixture of macromolecules isolated from mollusk shells; therefore, it is hard to single out one particular protein as being engaged in polymorph selection. Keene et al.⁸ investigated the interactions between the β -chitin and N-terminal peptide sequence of aragonite-associated protein (n16N), which is an IDP similar to Stm. It has been shown that n16N preferentially nucleates aragonite when it is bound to the β -chitin; otherwise, calcite is induced. Stm also probably has to interact with some other macromolecules to result in proper polymorph selection. Otolith matrix macromolecule-64 (OMM-64) from rainbow trout, which is a probable orthologue of Stm, requires otolin-1, a collagen-like protein, to induce aragonite formation *in vitro*. Neither OMM-64 nor otolin-1 induces aragonite.⁶² Structural similarities of OMM-64 and Stm may lead to a functional analogy in polymorph selection. The ability of an IDP to interact with

several different partners¹⁶ might predispose Stm to bind counterions as well as other framework proteins including otolin-1. Experiments with fluorescence-labeled proteins have proved that recombinant Stm and StmP are able to interact with calcium carbonate crystals. We propose that the protein is adsorbed on the surface of crystals and penetrates intergrain areas; however, it cannot be excluded that Stm penetrates the crystal lattice. Most likely, interactions of Stm and calcium and carbonate ions lead to the formation of definite polymorph forms and the shape and size of crystals. However, these interactions are not sufficient to induce aragonite. The synergistic effect of several macromolecules can switch the crystal polymorph, but it can also modulate the function of the protein. When they are in solution, DPP and DMP1 (just like Stm) can inhibit crystal nucleation and growth, while if DPP and DMP1 are adsorbed on a solid surface (for example collagen), they act as a template for crystal nucleation.⁵ Thus, the inhibitory activity may also be modulated by interactions with other macromolecules. Biominerization is a complex process involving a large number of macromolecules which are able to interact with each other. They are post-translationally modified in different ways, and this is crucial for the modulation of crystal growth functions. Certainly, there is still a lot of unknown information on protein-mediated biominerization. However, we believe that the intrinsic disorder of proteins involved in biominerization is a major functional advantage, because of the extensive flexibility of the polypeptide chains, which facilitates post-translational modifications and promotes numerous simultaneous interactions with several partners. Moreover, the inhibiting effects of protein on crystal growth is greatly dependent on the mobility of the protein.

AUTHOR INFORMATION

Corresponding Author

*Phone: 004871 320 63 40; fax: 004871 320 63 37; e-mail: piotr.dobryszycki@pwr.wroc.pl

ACKNOWLEDGMENT

This work was supported in part by the National Science Centre grant 1200/B/H03/2011/40 (to P.D.) and by Wrocław University Technology.

REFERENCES

- (1) Ross, M. D.; Pote, K. G. *Philos. Trans. R. Soc. London, B* **1984**, *1121*, 445–452.
- (2) Borelli, G.; Mayer-Gostan, N.; De Pontual, H.; Boeuf, G.; Payan, P. *Calcif. Tissue Int.* **2001**, *6*, 356–364.
- (3) Payan, P.; Edeyer, A.; de Pontual, H.; Borelli, G.; Boeuf, G.; Mayer-Gostan, N. *Am. J. Physiol.* **1999**, *1* (Pt 2), R123–31.
- (4) Boskey, A. L. *Connect. Tissue Res.* **2003**, *5*–9.
- (5) George, A.; Veis, A. *Chem. Rev.* **2008**, *11*, 4670–4693.
- (6) He, B.; Wang, K.; Liu, Y.; Xue, B.; Uversky, V. N.; Dunker, A. K. *Cell Res.* **2009**, *8*, 929–949.
- (7) Long, J. R.; Shaw, W. J.; Stayton, P. S.; Drobny, G. P. *Biochemistry* **2001**, *51*, 15451–15455.
- (8) Keene, E. C.; Evans, J. S.; Estroff, L. A. *Cryst. Growth Des.* **2010**, *3*, 1383–1389.
- (9) He, G.; Ramachandran, A.; Dahl, T.; George, S.; Schultz, D.; Cookson, D.; Veis, A.; George, A. J. *Biol. Chem.* **2005**, *39*, 33109–33114.
- (10) Sollner, C.; Burghammer, M.; Busch-Nentwich, E.; Berger, J.; Schwarz, H.; Riekel, C.; Nicolson, T. *Science* **2003**, *5643*, 282–286.
- (11) Hecker, A.; Testeniere, O.; Marin, F.; Luquet, G. *FEBS Lett.* **2003**, *1–3*, 49–54.
- (12) Kim, I. W.; Darragh, M. R.; Orme, C.; Evans, J. S. *Cryst. Growth Des.* **2006**, *1*, 5–10.
- (13) Feng, Q. L.; Pu, G.; Pei, Y.; Cui, F. Z.; Li, H. D.; Kim, T. N. J. *Cryst. Growth* **2000**, *1–4*, 459–465.
- (14) Kaplon, T. M.; Michnik, A.; Drzazga, Z.; Richter, K.; Kochman, M.; Ozyhar, A. *Biochim. Biophys. Acta* **2009**, *11*, 1616–1624.
- (15) Kaplon, T. M.; Rymarczyk, G.; Nocula-Lugowska, M.; Jakob, M.; Kochman, M.; Lisowski, M.; Szewczuk, Z.; Ozyhar, A. *Biomacromolecules* **2008**, *8*, 2118–2125.
- (16) Uversky, V. N.; Dunker, A. K. *Biochim. Biophys. Acta* **2010**, *6*, 1231–1264.
- (17) Tompa, P. *Curr. Opin. Struct. Biol.* **2011**, *3*, 419–425.
- (18) Uversky, V. N. *Protein J.* **2009**, *7–8*, 305–325.
- (19) Qin, C.; Baba, O.; Butler, W. T. *Crit. Rev. Oral Biol. Med.* **2004**, *3*, 126–136.
- (20) Verdelis, K.; Lukashova, L.; Yamauchi, M.; Atsawasawan, P.; Wright, J. T.; Peterson, M. G.; Jha, D.; Boskey, A. L. *Eur. J. Oral Sci.* **2007**, *4*, 296–302.
- (21) Xu, Y.; Zhang, H.; Yang, H.; Zhao, X.; Lovas, S.; Lundberg, Y. Y. *Dev. Dyn.* **2010**, *10*, 2659–2673.
- (22) Huq, N. L.; Cross, K. J.; Talbo, G. H.; Riley, P. F.; Loganathan, A.; Crossley, M. A.; Perich, J. W.; Reynolds, E. C. *J. Dent. Res.* **2000**, *11*, 1914–1919.
- (23) Milan, A. M.; Sugars, R. V.; Embrey, G.; Waddington, R. J. *Eur. J. Oral Sci.* **2006**, *3*, 223–231.
- (24) Gericke, A.; Qin, C.; Spevak, L.; Fujimoto, Y.; Butler, W. T.; Sorensen, E. S.; Boskey, A. L. *Calcif. Tissue Int.* **2005**, *1*, 45–54.
- (25) Panheleux, M.; Bain, M.; Fernandez, M. S.; Morales, I.; Gautron, J.; Arias, J. L.; Solomon, S. E.; Hincke, M.; Nys, Y. *Br. Poult. Sci.* **1999**, *2*, 240–252.
- (26) Veis, A.; Sfeir, C.; Wu, C. B. *Crit. Rev. Oral Biol. Med.* **1997**, *4*, 360–379.
- (27) Christensen, B.; Petersen, T. E.; Sorensen, E. S. *Biochem. J.* **2008**, *1*, 53–61.
- (28) Narayanan, K.; Ramachandran, A.; Hao, J.; He, G.; Park, K. W.; Cho, M.; George, A. J. *Biol. Chem.* **2003**, *19*, 17500–17508.
- (29) Mann, K.; Olsen, J. V.; Macek, B.; Gnäd, F.; Mann, M. *Proteomics* **2007**, *1*, 106–115.
- (30) Mann, K.; Poustka, A. J.; Mann, M. *Proteome Sci.* **2010**, *1*, 6.
- (31) Suzuki, Y.; Yamaguchi, A.; Ikeda, T.; Kawase, T.; Saito, S.; Mikuni-Takagaki, Y. *J. Dent. Res.* **1998**, *10*, 1799–1806.
- (32) Lasa, M.; Chang, P. L.; Prince, C. W.; Pinna, L. A. *Biochem. Biophys. Res. Commun.* **1997**, *3*, 602–605.
- (33) Kim, I. W.; DiMasi, E.; Evans, J. S. *Cryst. Growth Des.* **2004**, *6*, 1113–1118.
- (34) Takeuchi, T.; Sarashina, I.; Iijima, M.; Endo, K. *FEBS Lett.* **2008**, *5*, 591–596.
- (35) Hecker, A.; Quennedey, B.; Testeniere, O.; Quennedey, A.; Graf, F.; Luquet, G. *J. Struct. Biol.* **2004**, *3*, 310–324.
- (36) Addadi, L.; Weiner, S. *Proc. Natl. Acad. Sci. U.S.A.* **1985**, *12*, 4110–4114.
- (37) Lakshminarayanan, R.; Valiyaveettil, S.; Rao, V. S.; Kini, R. M. *J. Biol. Chem.* **2003**, *5*, 2928–2936.
- (38) Laemmli, U. K. *Nature* **1970**, *5259*, 680–685.
- (39) Lowry, O. H.; Rosebrough, N. J.; Farr, A. L.; Randall, R. J. *J. Biol. Chem.* **1951**, *1*, 265–275.
- (40) Gower, L. B.; Odom, D. J. *J. Cryst. Growth* **2000**, *4*, 719–734.
- (41) Wolf, S. E.; Leiterer, J.; Pipich, V.; Barrea, R.; Emmerling, F.; Tremel, W. *J. Am. Chem. Soc.* **2011**, *32*, 12642–12649.
- (42) Tohse, H.; Takagi, Y.; Nagasawa, H. *FEBS J.* **2008**, *10*, 2512–2523.
- (43) Hughes, I.; Blasile, B.; Huss, D.; Warchol, M. E.; Rath, N. P.; Hurle, B.; Ignatova, E.; Dickman, J. D.; Thalmann, R.; Levenson, R.; Ornitz, D. M. *Dev. Biol.* **2004**, *2*, 391–402.
- (44) Bajoghli, B.; Ramialisson, M.; Aghaallaei, N.; Czerny, T.; Wittbrodt, J. *Dev. Dyn.* **2009**, *11*, 2860–2866.

- (45) Kang, Y. J.; Stevenson, A. K.; Yau, P. M.; Kollmar, R. *J. Assoc. Res. Otolaryngol.* **2008**, *4*, 436–451.
- (46) Murayama, E.; Herbomel, P.; Kawakami, A.; Takeda, H.; Nagasawa, H. *Mech. Dev.* **2005**, *6*, 791–803.
- (47) Lasa, M.; Chang, P. L.; Prince, C. W.; Pinna, L. A. *Biochem. Biophys. Res. Commun.* **1997**, *3*, 602–605.
- (48) Ali, A.; Hoeflich, K. P.; Woodgett, J. R. *Chem. Rev.* **2001**, *8*, 2527–2540.
- (49) Iakoucheva, L. M.; Radivojac, P.; Brown, C. J.; O'Connor, T. R.; Sikes, J. G.; Obradovic, Z.; Dunker, A. K. *Nucleic Acids Res.* **2004**, *3*, 1037–1049.
- (50) Lee, S. L.; Veis, A.; Glonek, T. *Biochemistry* **1977**, *16*, 2971–2979.
- (51) Lewit-Bentley, A.; Rety, S. *Curr. Opin. Struct. Biol.* **2000**, *6*, 637–643.
- (52) Fekete, D. M. *Science* **2003**, *5643*, 241–242.
- (53) Inoue, H.; Ohira, T.; Nagasawa, H. *Peptides* **2007**, *3*, 566–573.
- (54) Fu, G.; Valiyaveettil, S.; Wopenka, B.; Morse, D. E. *Biomacromolecules* **2005**, *3*, 1289–1298.
- (55) Ren, D.; Feng, Q.; Bourrat, X. *Micron* **2011**, *3*, 228–245.
- (56) Levi, Y.; Albeck, S.; Brack, A.; Weiner, S.; Addadi, L. *Chem.—Eur. J.* **1998**, *3*, 389–396.
- (57) Kono, M.; Hayashi, N.; Samata, T. *Biochem. Biophys. Res. Commun.* **2000**, *1*, 213–218.
- (58) Samata, T.; Hayashi, N.; Kono, M.; Hasegawa, K.; Horita, C.; Akera, S. *FEBS Lett.* **1999**, *1–2*, 225–229.
- (59) Lippmann, F. *Sedimentary carbonate minerals*; Springer-Verlag: New York, 1973.
- (60) Raz, S.; Weiner, S.; Addadi, L. *Adv. Mater.* **2000**, *1*, 38–42.
- (61) Falini, G.; Albeck, S.; Weiner, S.; Addadi, L. *Science* **1996**, *5245*, 67–69.
- (62) Tohse, H.; Saruwatari, K.; Kogure, T.; Nagasawa, H.; Takagi, Y. *Cryst. Growth Des.* **2009**, *11*, 4897–4901.